Re-examining the *XMM–Newton* spectrum of the black hole candidate XTE J1652−453

Chia-Ying Chiang,[1][*] R. C. Reis,[2] D. J. Walton[1] and A. C. Fabian[1]

[1]*Institute of Astronomy, University of Cambridge, Madingley Road, Cambridge CB3 0HA*
[2]*Department of Astronomy, University of Michigan, 500 Church Street, Ann Arbor, MI 48109, USA*

ABSTRACT

The *XMM–Newton* spectrum of the black hole candidate XTE J1652−453 shows a broad and strong Fe Kα emission line, generally believed to originate from reflection of the inner accretion disc. These data have been analysed by Hiemstra et al. using a variety of phenomenological models. We re-examine the spectrum with a self-consistent relativistic reflection model. A narrow absorption line near 7.2 keV may be present, which if real is likely the Fe XXVI absorption line arising from highly ionized, rapidly outflowing disc wind. The blueshift of this feature corresponds to a velocity of about $11\,100\,\mathrm{km\,s^{-1}}$, which is much larger than the typical values seen in stellar mass black holes. Given that we also find the source to have a low inclination ($i \lesssim 32°$; close to face-on), we would therefore be seeing through the very base of outflow. This could be a possible explanation for the unusually high velocity. We use a reflection model combined with a relativistic convolution kernel which allows for both prograde and retrograde black hole spin, and treat the potential absorption feature with a physical model for a photoionized plasma. In this manner, assuming the disc is not truncated, we could only constrain the spin of the black hole in XTE J1652−453 to be less than $\sim 0.5\,Jc/GM^2$ at the 90 per cent confidence limit.

Key words: accretion, accretion discs – black hole physics – X-rays: binaries.

1 INTRODUCTION

Black hole binaries (BHBs) are known to exhibit a number of active accretion states, each with different spectral and timing characteristics. Amongst these, the most prominent are the low/hard state, dominated by hard power-law-like emission which most likely arises due to Compton scattering, and the thermal-dominated state, where the X-ray spectrum displays the strong presence of thermal emission from an optically thick accretion disc. Between these two well-known states lie a number of intermediate states, in which the Comptonized emission and the thermal disc can contribute comparable amounts to the radiated flux (see Homan et al. 2001; Remillard & McClintock 2006, for a full description of spectral states in BHBs).

It is often found that, in addition to this X-ray continuum, the spectra of accreting black holes – both stellar mass ($M_{\mathrm{BH}} \sim 10\,\mathrm{M_{\odot}}$) and supermassive ($M_{\mathrm{BH}} \gtrsim 10^5\,\mathrm{M_{\odot}}$) black holes – display the presence of reflection features, arising through irradiation of the 'cold' accretion disc by the high-energy Comptonized X-rays. Of these, the Fe Kα line is usually the most prominent feature. Although

this feature is atomic in nature and hence intrinsically narrow, the observed iron emission line is often found to be very broad due to a combination of the Doppler effect and gravitational redshift close to the black hole (Fabian et al. 1989). The first observational detection of a broad Fe Kα line was found in the X-ray spectrum of the type 1 active galactic nucleus (AGN) MCG−6-30-15 (Tanaka et al. 1995), and such features have since been seen in a very large number of objects ranging from neutron stars (Bhattacharyya & Strohmayer 2007; Cackett et al. 2009a,b; di Salvo et al. 2009; Reis, Fabian & Young 2009b) to stellar mass black holes (Miller 2007; Blum et al. 2009; Reis et al. 2009a; Hiemstra et al. 2011) to AGNs (Tanaka et al. 1995; Fabian et al. 2009; Miniutti et al. 2009; Schmoll et al. 2009; Brenneman et al. 2011; Reis et al. 2011). Furthermore, Walton et al. (2012) highlight the similarity of the broadened iron lines observed in BHBs and active galaxies, strongly supporting a relativistic disc reflection origin. Due to the fact that these lines are emitted from regions close to the central black hole, their profile offers information of the innermost regions of the accretion flow, and can be used to determine the inner radius of the accretion disc from which black hole spin can be inferred, under the assumption that this radius represents the innermost stable circular orbit (ISCO; Bardeen, Press & Teukolsky 1972). The other major signature of reflection is the Compton hump, a broad emission feature at

[*]E-mail: cychiang@ast.cam.ac.uk

~30 keV which arises due to the relative interplay of photoelectric absorption of low-energy photons and Compton down scattering of high-energy photons within the reflecting medium. This feature is also frequently observed in both stellar mass and supermassive black holes (see e.g. Zdziarski, Lubiński & Smith 1999; Zdziarski et al. 2002; Miniutti, Fabian & Miller 2004; Cadolle Bel et al. 2007; Reis, Fabian & Miller 2010; Walton, Reis & Fabian 2010; Chiang & Fabian 2011).

Being largely atomic in nature, reflection features are independent of black hole mass, providing the ideal method to measure spin in both stellar mass black holes and their supermassive counterparts. It is also possible to measure the inner radius of the disc through direct study of the thermal disc emission, but detailed knowledge of the black hole mass and its distance are required (Zhang, Cui & Chen 1997; Davis, Done & Blaes 2006; McClintock et al. 2006). Recently, Steiner et al. (2009) have shown that both the reflection features and the thermal continuum give similar estimates for the spin of the BHB XTE J1550−564, undertaking one of the first major attempts at cross-calibrating these two methods.

In addition to these emission processes, if there is substantial intervening material along our line of sight to the black hole, this will imprint absorption features on to the observed X-ray spectrum. Complex absorption features are observed relatively frequently in both AGNs and X-ray binaries, although with somewhat varying properties. In the latter case, the material usually appears to be highly ionized and outflowing, suggesting an origin in some kind of wind launched from the inner regions of the accretion flow; for an excellent example, see the *Chandra* and *XMM–Newton* grating observations of the Galactic black hole transient GRO J1655−40 presented by Miller et al. (2006).

XTE J1652−453 is a new X-ray transient discovered as part of the *RXTE* Galactic bulge scan performed in 2009 (Markwardt et al. 2009a). Later observations by the *Swift* and *RXTE* indicate the source is likely a black hole candidate (Markwardt et al. 2009b). Simultaneous *XMM–Newton* and *RXTE* observations were taken during the decay of the 2009 outburst, in which the source was found to be in a hard-intermediate state, and originally presented by Hiemstra et al. (2011). These data show clear evidence for a strong and broad iron emission feature and, through considering a variety of physically motivated – albeit largely phenomenologically modelled – interpretations, the authors concluded that the accretion disc must extend as far in as ~4 gravitational radii ($R_G = GM/c^2$) from the central black hole. Under the standard assumption that this is the ISCO, this radius equates to a spin of ~0.5, although Hiemstra et al. (2011) argue that the disc may in fact be truncated at a radius larger than the ISCO and that this should be considered as a lower limit to the intrinsic spin of the system. A further curiosity unearthed by these authors is that, when using the fully self-consistent reflection code REFLIONX (Ross & Fabian 2005) to account for the line profile, the best-fitting model showed the presence of a possible ionized absorption feature at ~7.2 keV, which although considered briefly, was ultimately dismissed as a potential deficiency in the model.

The purpose of the present work is to revisit the spin constraint obtained for XTE J1652−453 with the advent of the REFBHB (Ross & Fabian 2007) reflection model, which is self-consistently calculated for use with high-temperature accretion discs present in BHB systems, and to investigate whether accounting for the absorption-like feature in a physical manner has any effect on this result. The paper is structured as follows: Section 2 briefly outlines the data reduction, Section 3 details our analysis of the broad-band spectrum, Section 4 discusses the results obtained and finally Section 5 summarizes our conclusions.
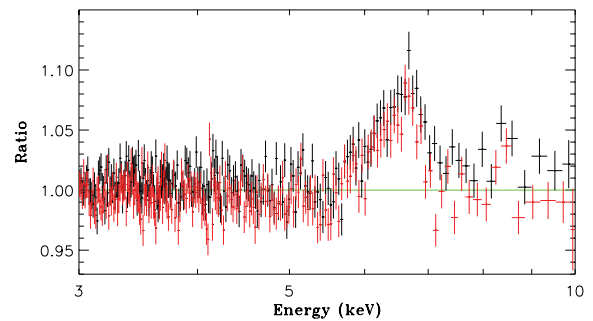
Figure 1. The broad Fe line in the *XMM–Newton* PN spectrum of XTE J1652−453. The black data points present the spectrum without the CTI corrections, while the red ones stand for the CTI-corrected spectrum. A mild gain shift between these spectra can been seen in the figure. The line profiles in the spectra are almost identical. The small peak around ~8 keV comes from the background.

2 DATA REDUCTION

We reduced the *XMM–Newton* data using the Science Analysis Software (SAS) 10.0.1 with the latest calibration files. The European Photon Imaging Camera (EPIC) PN was operated in timing mode, and we extracted source spectrum of the PN data using the RAWX columns in [30:46] following the standard procedures and the initial work by Hiemstra et al. (2011). As was shown by these authors, the wings of the source point spread function extend beyond the CCD boundaries and therefore there are no areas in the chip that is source free from which a background can be taken. However, Hiemstra et al. (2011) investigated in detail the effect of different background models and concluded that this has little influence in any of the fit parameters of interest. For this reason we follow from their work and do not use a background and add the further note that the source count rate is over 200 times higher than that of the contaminated background.

As the EPIC-PN detector was operated in the fast-readout timing mode, the effects of charge transfer inefficiency (CTI) and/or X-ray loading may not have been properly accounted for by the standard reduction pipeline,[1] resulting in a mismatch between the energies of the instrumental edges (~2 keV) in the data and in the response matrices. Although strong residuals are not observed around these features in this case, the previous work on this source attempted to correct for any potential calibration uncertainties that remain with the EPFAST tool. However, as demonstrated by Walton et al. (2012), the application of EPFAST can result in an incorrect energy scale at high energies, particularly around the iron line. Therefore, we test briefly whether this tool has any strong effects on the results obtained. We find that in this case, owing to the much lower source count rate, EPFAST does not apply any significant correction, and the unmodified and EPFAST-modified data are fully consistent, as shown by Fig. 1. However, owing to the presence of an unidentified excess below 1.5 keV (such features are frequently seen in timing mode observations[1]), we only fit the PN data above 2.2 keV and use the Reflection Grating Spectrometer (RGS) between 0.4 and 2.0 keV, similar to the approach taken by Hiemstra et al. (2011). Similarly, we also used the *RXTE* Standard-2 data between 7 and 20 keV and the High Energy X-ray Timing Experiment (HEXTE) data between 20 and 200 keV, allowing for a constant of normalization between all different spectra.

[1] See http://xmm2.esac.esa.int/docs/documents/CAL-TN-0083.pdf

3 DATA ANALYSIS AND RESULTS

As mentioned in Section 1, the *XMM–Newton* spectrum of XTE J1652−453 shows a broad, skewed line profile (see Fig. 1) that is likely reflected emission from the inner part of the accretion disc around the black hole. We refer the reader to Hiemstra et al. (2011) for a detailed analysis of this source using a variety of phenomenological models. To cross-check with their results, we begin by reproducing the final model presented in that work, which consists of a power-law continuum, a thermal disc component (DISKBB; Mitsuda et al. 1984) and relativistic disc reflection. The latter component is modelled with the REFLIONX reflection code (Ross & Fabian 2005), with the relativistic effects provided by the KERRCONV (Brenneman & Reynolds 2006) convolution kernel. Galactic absorption is also included, initially modelled with the PHABS photoelectric absorption code, with N_H free to vary, and we also include the additional absorption components originally used by Hiemstra et al. (2011). We obtained a spin parameter of ~0.5 ± 0.2, in excellent agreement with the published result, and the other parameters in the model also agree well within statistical errors. The ~7.2 keV absorption line which has been reported by the authors is also present in our spectrum. As previously mentioned, this feature was dismissed as a potential deficiency in the model. In order to check the validity of this claim, we proceed by modelling the broad-band continuum with a physically self-consistent model including the latest reflection and relativistic convolution models.

First, we replaced the Galactic absorption model PHABS with the latest high-resolution model TBNEW[2] (Wilms et al., in preparation), using the new solar abundances presented in that work. We then replaced the REFLIONX reflection model with REFBHB (Ross & Fabian 2007), and the KERRCONV convolution kernel with RELCONV[3] (Dauser et al. 2010). The REFBHB reflection model has been calculated specifically for use with BHB systems, allowing for a hot accretion disc as opposed to the cool disc temperature with which REFLIONX was calculated, and including the thermal emission from this component self-consistently both in the spectrum and when determining the disc ionization. The key free parameters of REFBHB are the photon index of the illuminating continuum (Γ), which is required to be the same as the power-law continuum, the black-body temperature of the accretion disc (kT), the surface hydrogen density of the accretion disc (n_H) and the ratio of the illuminating to the blackbody fluxes (F_{ill}/F_{th}). The RELCONV convolution model is very similar to KERRCONV, but this model also allows for a retrograde spin parameter. We make use of this code assuming the limb-darkening effects outlined by Laor (1991). Note that, owing to the lack of background correction, we also include an unresolved Gaussian feature at 8.1 keV to account for the well-known instrumental Copper feature.[4] With this new model (hereafter model A), we find that the extra absorption component at ~1.4 keV mentioned in Hiemstra et al. (2011) is not obvious in our fit, although the potential absorption features at ~7.2 and ~10 keV are still present. This model otherwise provides a good fit to the data, as shown in Fig. 2, and the results obtained are presented in Table 1. We also include the results obtained by Hiemstra et al. (2011) with the DISKBB+REFLIONX combination for ease of comparison.

There are some differences between our results and those of Hiemstra et al. (2011). We obtained a higher Galactic absorption
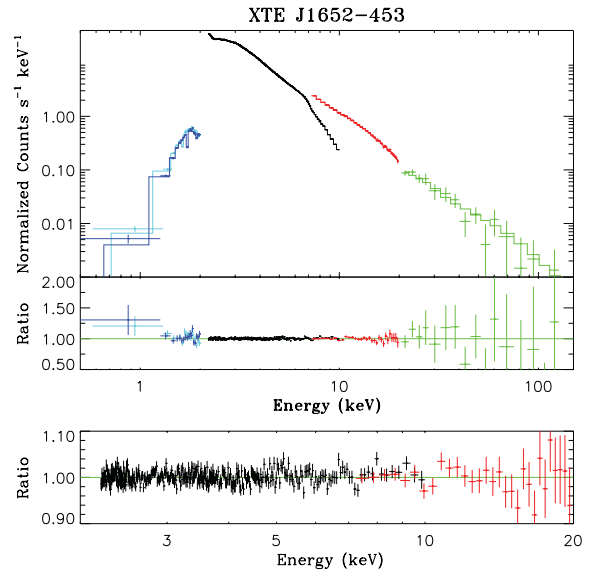
Figure 2. The best fit of the simultaneous *XMM–Newton* and *RXTE* observations using model A. The black data points in the upper panel belong to the PN spectrum, while the blue and cyan ones are of RGS1 and RGS2, the red and green ones are of the *PCA* and HEXTE spectrum, respectively. The lower panel shows the data/model ratio of the fitting. Data points are rebinned for clarity.

column N_H and a harder photon index Γ, although the former at least is likely to be due to the different reflection model used in our work. We obtain a good agreement between the disc temperatures, as the temperature obtained with REFBHB is the effective disc temperature, which is known to be a factor of ~1.7 (Shimura & Takahara 1995) less than the surface (or 'colour') temperature obtained when using DISKBB. The values of the emissivity profile index obtained in our models are also in close agreement. The spin constraint of $a^* = 0.13 \pm 0.29$ obtained here, the main focus of this work, is much weaker than that originally presented by Hiemstra et al. (2011) ($a^* = 0.45 \pm 0.02$).

3.1 Potential absorption in the Fe K band

The potential absorption features at ~7.2 and ~10 keV were both originally reported by Hiemstra et al. (2011). In order to investigate the statistical significance of these features with our new model, we added an inverse narrow (line width =10 eV) Gaussian line, and systematically varied the line energy between 6.4 and 11 keV in 60 steps. In Fig. 3 we plot the $\Delta\chi^2$ improvement gained with the addition of the narrow line as a function of the line energy. The potential features at 7.2 and 9.7 keV are clearly picked out, although their overall detection significances are not particularly high. The feature at 7.2 keV has the strongest detection significance of the two, but we estimate that this is only just greater than 2σ; the equivalent width obtained is EW $= -20^{+13}_{-15}$ eV. If real, the most likely association of this feature is highly ionized iron absorption arising in some outflowing disc wind. The closest transition is Fe XXVI Kα at 6.97 keV, although this would imply an outflow velocity of ~11 000 km s^{-1}, much higher than typically observed for BHB disc winds (see e.g. Miller et al. 2006). Unfortunately, we were unable to find a suitable atomic association for the feature at 9.7 keV that would imply a similar outflow velocity, so the nature and velocity (and even the presence) of the outflow remain unconfirmed. Furthermore, since

[2] http://pulsar.sternwarte.uni-erlangen.de/wilms/research/tbabs/
[3] http://www.sternwarte.uni-erlangen.de/~dauser/research/relline/index.html
[4] http://xmm.vilspa.esa.es/docs/documents/CAL-TN-0068-0-1.ps.gz

Table 1. The fitting parameters from different model components and χ^2 obtained by different models. The Galactic absorption column N_H is given in $10^{22}\,cm^{-2}$. The index stands for the emissivity profile index in the convolution model (RELCONV for models A–C and KERRCONV for the work by Hiemstra et al. 2011), and a^* and i stand for the spin parameter and the inclination angle, respectively. The absorption column N_{iH} of the absorbing component is also given in $10^{22}\,cm^{-2}$, while the ionization parameter ξ is in $erg\,cm\,s^{-1}$. n_H, kT and F_{ill}/F_{th} are parameters of the REFBHB component. The emissivity index has been set to be 0 for the inner part of the accretion disc and 3 for the outer region.

Parameter	Model A	Model B	Model C	Hiemstra et al.
N_H ($10^{22}\,cm^{-2}$)	$7.07^{+0.07}_{-0.10}$	7.02 ± 0.11	7.01 ± 0.10	6.73 ± 0.01
Γ	$2.10^{+0.02}_{+0.05}$	$2.09^{+0.03}_{-0.04}$	$2.09^{+0.03}_{-0.04}$	2.16 ± 0.02
Index	$2.6^{+0.0}_{-0.3}$	$3.1^{+0.4}_{-0.3}$	Fixed^a	2.7 ± 0.1
R_{bk} (R_G)	–	–	$9.1^{+4.0}_{-2.3}$	–
a^*	0.13 ± 0.29	$\lesssim 0.6$	Unconstrained	0.45 ± 0.02
i	$\lesssim 14°$	$28° \pm 3°$	$28°^{+3}_{-2}$	$8°\!.8 \pm 0°\!.1$
N_{iH} ($10^{22}\,cm^{-2}$)	–	>2.3	>2.2	–
$\log \xi$	–	>3.94	>3.96	–
z	–	$-0.036^{+0.008}_{-0.006}$	$-0.036^{+0.008}_{-0.005}$	–
n_H ($10^{19}\,cm^{-2}$)	$5.2^{+0.3}_{-0.6}$	$7.7^{+3.0}_{-2.2}$	$7.6^{+1.5}_{-2.3}$	–
kT (keV)	0.38 ± 0.01	0.38 ± 0.01	0.38 ± 0.01	0.59 ± 0.01
F_{ill}/F_{th}	0.6 ± 0.1	0.5 ± 0.1	0.5 ± 0.1	–
χ^2_ν (χ^2/d.o.f.)	1.04 (2177.6/2095)	1.04 (2164.1/2092)	1.04 (2164.5/2092)	1.26 (460.2/365)

^{a}A broken emissivity profile has been used in this model.
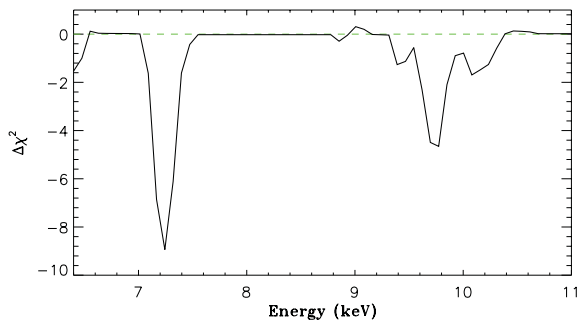
Figure 3. A search of energy space between 6.4 and 11 keV when fitting a narrow (10 eV) inverse Gaussian line to the spectrum. The y-axis shows the amount of χ^2 changed after putting the inverse line.

this second feature does not affect the Fe K band, which is the primary focus of this work, we will not consider it further.

Regardless of the strict statistical significance of the potential Fe XXVI absorption line, we wish to investigate what effect modelling this feature in a physical manner has on the spin constraint obtained. We therefore generated an ionized absorption model using the XSTAR photoionization code (v2.2.0). The ionizing continuum was assumed to have a power-law shape over the 0.1–20 keV energy range, and we adopted an ionizing luminosity (1–1000 Ryd) of $10^{38}\,erg\,s^{-1}$, a typical value for bright stellar mass black holes (the distance to this source is not yet well constrained). The temperature of the photoionized gas was fixed at 10^5 K, the turbulent velocity v_{turb} at 150 km s^{-1} and the iron abundance at the solar value. The free parameters of the generated model are the photon index of the ionizing continuum, which was required to be the same as the power-law continuum component, the absorbing column density (N_H), the ionization parameter ($\log \xi$) and the outflow velocity (in the form of the redshift of the gas, z). We also tested an absorption model in

which the assumed ionizing continuum had a thermal shape, but the results obtained with these two models were in excellent agreement, so we only present the former case.

We added this absorption component to the model including REF-BHB constructed above and re-fit the spectra (this shall hereafter be referred to as model B). This model of course fits the data well, and the results obtained are also quoted in Table 1. The absorbing gas is highly ionized, in accordance with the lack of absorption features in the RGS spectrum, and, as demonstrated by Fig. 4, only contributes the absorption line at 7.2 keV.

Models A and B yield similar results in most of the fitting parameters. However, when we include the photoionized absorber to account for the possible Fe XXVI feature at 7.2 keV, while there is a local minimum consistent with the result obtained by Hiemstra et al. (2011) and similar to the result obtained with model A, we find that the globally preferred solution has a maximal retrograde spin, with an upper limit of $a^* \lesssim -0.4$. Fig. 5 shows the 1D χ^2 confidence contours for the spin parameter in both cases. A further difference is the value of the inner disc inclination. The inclination obtained with the basic reflection model, $i < 14°$, is consistent with the previously published result, but the inclusion of the ionized absorber changes the inclination to $i = 28° \pm 3°$, although there are also a series of local minima at lower inclinations. Fig. 6 shows the 1D χ^2 confidence contours for the disc inclination for both cases.

These changes suggest there may be some degeneracies between the values obtained for the spin and the inclination of the system. Indeed, degeneracies in the blurring parameters have been found to be an issue during the application of reflection models to a number of other sources (see e.g. Nardini et al. 2011). In order to fully investigate this possibility, we show the 2D confidence contours in the spin–inclination parameter space for model B in Fig. 7. The global minimum associated with a maximum retrograde spin and indicated with a bold cross is associated with a higher inclination, while the local minimum at an intermediate prograde spin is
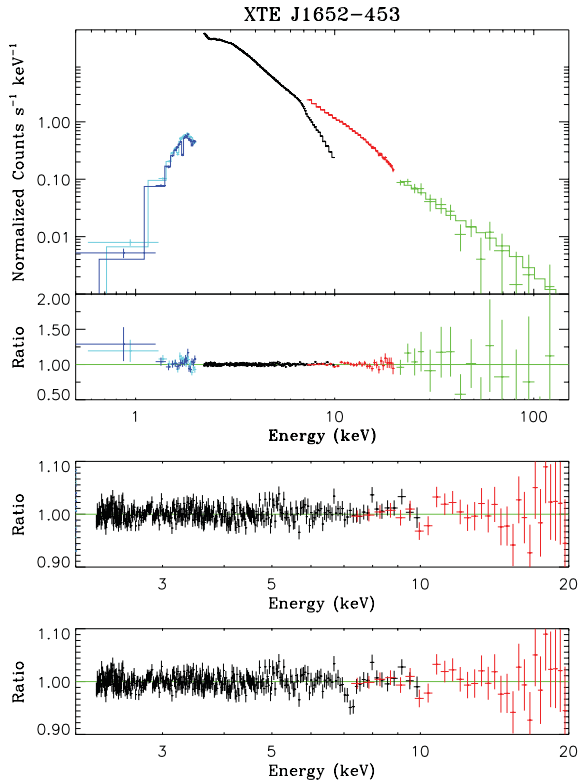
Figure 4. The upper part of the figure shows the result fitted the data sets with model B. The middle part shows the zoom-in data/model ratio from 2 to 20 keV, while the lower part of the figure shows the data/model ratio of the same energy range when the warm absorber is taken out from model B. It can be clearly seen that the absorbing zone only produces the absorption line around 7.2 keV.
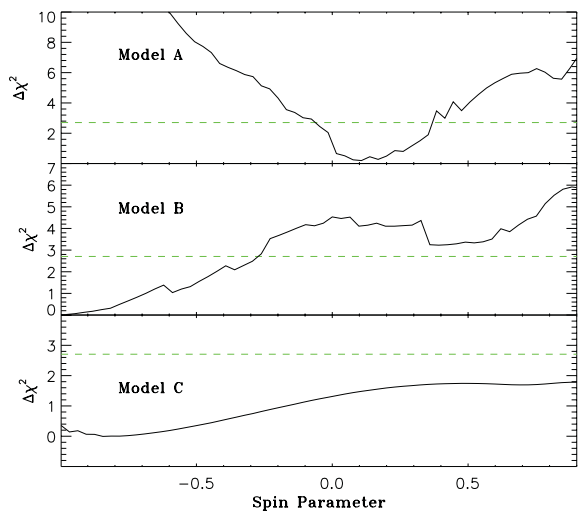
Figure 5. The goodness-of-fit versus spin parameter for XTE J1652−453 with models A–C, from top to bottom. The global minimum of model B indicates a maximally rotating retrograde black hole. However, see degeneracies shown in Fig. 7. Model C does not give a constrained value of the spin parameter.
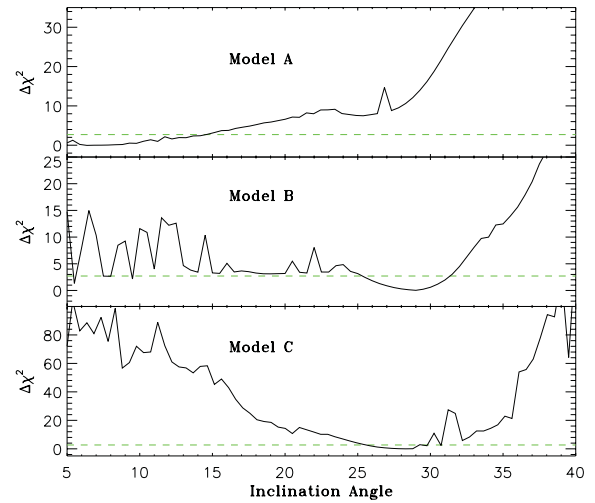
Figure 6. Goodness-of-fit versus inclination angle of models A–C. For model A an inclination angle $i \lesssim 14°$ is preferred. A global minimum of approximately $28°$ has been found with model B. However, note a series of local minima located below $10°$. An inclination $>35°$ is rejected at greater than the 3σ level.
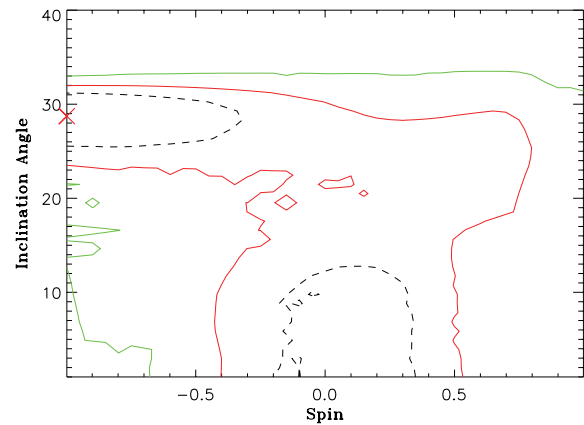
Figure 7. The contour plot of the spin parameter against the inclination angle of model B. The 90 per cent contours span a wide range, indicating the possible spin parameter could be any value $\lesssim 0.8$. The red cross shows the best-fitting set of values by model B.

associated with a lower inclination. This would appear to confirm that there is indeed a mild degeneracy between these parameters. Given that it is not clear whether the feature at 7.2 keV is real or simply a statistical fluctuation, the only limit on the spin we can place with any confidence is $a^* \lesssim 0.5$, although a maximum retrograde spin remains a very intriguing possibility.

3.2 Large scale height corona

An alternative geometry to a compact corona close to the event horizon is the possibility that the corona is located at a large vertical height from the accretion disc. In this scenario, the emissivity index is expected to be flat up to a break radius (Vaughan et al. 2004) where beyond this it reverts to the traditional Newtonian value of 3. Such geometry, if not properly accounted for, could potentially mimic a truncated accretion disc or a retrograde spin. We test this possibility by setting the inner emissivity index in model B to be 0 up to a break radius (R_{bk}) and 3 beyond that. This fit (model C, Table 1) yields a break radius of $\sim 10 R_G$, which suggests that the

corona is located at a similar vertical distance, and provides an equally good fit (reduced $\chi^2 = 2164.5/2092$) to model B. From Fig. 5 we can see that the spin parameter is unconstrained if the corona is assumed to be at a large scale height.

4 DISCUSSION

We have re-analysed the simultaneous *XMM–Newton* and *RXTE* spectra of the BHB candidate XTE J1652−453 obtained during the recent outburst displayed by this source in 2009. Our work focuses in particular on the relativistically broadened iron emission, with the purpose of making use of the new REFBHB reflection model to constrain the spin of the black hole. The previous spin constraint of $a^* = 0.45 \pm 0.02$, published by Hiemstra et al. (2011), made use of the REFLIONX reflection model, which is calculated for use primarily with AGN. We also make use of the new convolution kernel RELCONV, which accounts for the relativistic effects present in the regions close to a black hole, and crucially allows for black hole spins that are retrograde with respect to the material orbiting in the accretion disc. The decomposed components of the model have been shown in Fig. 8.

We find first of all that, when using this new reflection model, the constraint on the black hole spin obtained, $a^* = 0.13 \pm 0.29$, is much looser than the previously published result. This most likely reflects the differing scenarios for which REFBHB and REFLIONX were created. Although the same physics and atomic data are included in both models, the former allows the disc temperature to be varied in a range suitable for the hot discs around BHBs, while the latter assumes a cool disc temperature of $kT = 10$ eV, more suitable for the discs around AGNs. These higher temperatures naturally lead to a highly ionized disc and a more significant contribution to the bredth of the observed emission line from Compton scattering during the reflection process, as Compton broadening becomes more important as the temperature of the scattering electrons (and hence the disc temperature) increases (Pozdnyakov, Sobol & Syunyaev 1983). Furthermore, we also found that there is a mild degeneracy between the black hole spin and the disc inclination, with higher inclinations broadly leading to solutions with higher black hole spin. The combination of these factors naturally make it more difficult to strongly constrain the black hole spin and lead to the updated constraints obtained in this work being less restrictive.
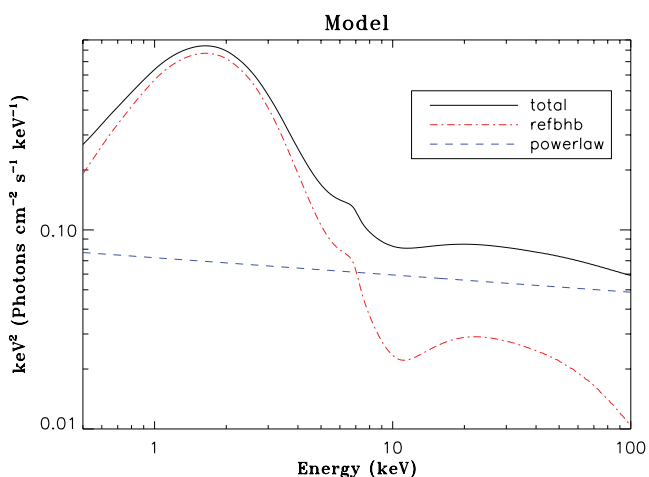
Figure 8. The main decomposed components of the model used in this work. The total model is shown in black curve. Absorption components have been removed from this figure.

Inspecting the residuals after modelling the spectrum with the basic disc reflection interpretation, we confirmed the possible existence of a narrow absorption feature at 7.2 keV. This was originally highlighted by Hiemstra et al. (2011), but dismissed as a deficiency in the model used in that work. The persistence of this potential feature when using the best physically self-consistent BHB reflection model currently available suggests that other explanation should be pursued. We stress that the inclusion of a Gaussian absorption feature only leads to a marginal improvement in terms of the quality of fit, so we do not consider the detection of this feature to be formally significant, and wish to reiterate the strong possibility that it merely arises through statistical fluctuations. However, it is also important to consider what effect this potential feature might have on the spin constraint obtained. With the inclusion of an ionized absorption component, produced with the XSTAR photoionization code, we find that the spin can only be constrained to be $a^* \lesssim 0.6$ (when considering the 90 per cent confidence contour for the combination of spin and inclination). This difference most likely arises due to the mild degeneracy between the spin and inclination mentioned earlier (shown in Fig. 7). The energy at which the residuals are seen is roughly coincident with the blue wing of the emission line, which is the region of the line profile that has the strongest influence on the inclination obtained. The inclusion of this feature in the model changes the inclination, and hence changes the spin constraint.

A black hole spinning in a retrograde manner with respect to the orbital motion of its accretion disc is a very interesting and unusual prospect. Retrograde spin can result in a large gap between the ISCO and the event horizon, in which magnetic fields can gather and provide forces to power a jet. In fact, there have been claims that retrograde spin may launch stronger outflows than prograde spin (e.g. Garofalo 2009; Garofalo, Evans & Sambruna 2010; however, see De Villiers et al. 2005; Tchekhovskoy & McKinney 2012). Of course, the possible retrograde spin obtained with model B depends not only on the assumption that the potential absorption feature is real, but also on the assumption that the inner radius of the accretion disc is coincident with the ISCO of the black hole. It is well accepted that at low accretion rates, the inner disc actually truncates at some distant radius from the ISCO, although the exact point at which this begins to happen is still hotly debated (e.g. Reis et al. 2010). The retrograde spin constraint obtained could simply imply instead that the source was observed when the disc was mildly truncated ($R_{in} \sim 10 R_G$).

If the 7.2-keV absorption feature is real, its most likely identification is a blueshifted Fe XXVI absorption line arising in an outflowing disc wind, although the outflow velocity of $v_{out} \sim 10\,000$ km s^{-1} implied is substantially higher than the velocities of $\lesssim 1000$ km s^{-1} typically observed from winds in BHBs. Nevertheless, the energy of the line is not high enough for an identification with nickel, and invoking any other iron transition would require an even higher outflow velocity. Outflow velocities of this order, or even larger, have frequently been claimed in active galaxies (see e.g. Pounds & Reeves 2009; Reeves et al. 2009; Tombesi et al. 2010), and there has more recently been a detection of a similarly fast outflow in the BHB candidate IGR J17091−3624 (King et al. 2012).

The slower disc winds more frequently observed in BHBs are observed predominantly at high disc inclinations, when we are observing the source close to an edge-on orientation. However, our modelling would suggest this is not actually the case for XTE J1652−453. In this context, a relatively weak line with an unusually high outflow velocity might not be so surprising; most numerical simulations of equatorial disc winds suggest that both the density and outflow velocity of such outflows evolve with the inclination at which they are observed, with the winds appearing

more tenuous but with higher outflow velocities when observed at low inclinations (see e.g. Proga & Kallman 2002). An interesting alternative origin for the large energy shift of this potential feature was recently proposed by Gallo & Fabian (2011), who demonstrate that if the absorbing material originates close to the black hole and orbits with the accretion disc (as would be expected for a wind launched from the disc), the same effects that skew the emission from this region can also result in large shifts in the observed energies of absorption features. However, in order to produce a narrow feature in this way, the absorbing material may need to be confined to a relatively narrow range of radii.

We have also investigated the possibility that the Comptonizing corona could actually have a large scale height above the plane of the accretion disc (model C). In this scenario, we find that the spin cannot be constrained. The primary constraint on the black hole spin comes from the extent of the red wing in the iron emission line, which is directly related to the inner disc radius. Different emissivities result in different iron line profiles, with higher emissivity indices giving rise to stronger (but not more extended red wings) emission at lower energies compared to low-emissivity indices. The low-emissivity index assumed in this scenario naturally makes it more difficult to constrain the spin given the low signal-to-noise ratio in the present data.

5 CONCLUSION

We have analysed the simultaneous *XMM–Newton* and *RXTE* data of the black hole candidate XTE J1652−453. The spectra have been modelled using a sophisticated model which consists of a power-law continuum and a reflection component. We used the REFBHB model, which is appropriate for stellar mass black holes, to model the reflected continuum. The convolution model we use allows for the possibility of retrograde spins. The possibility of a weak absorption line at ∼7.2 keV has been confirmed. Assuming this feature is real, it is likely associated with a blueshifted Fe XXVI line, having an outflow velocity of $\sim 11\,100\ \mathrm{km\,s^{-1}}$, which is much higher than the general value seen in stellar mass black holes, and is similar to the newly found source IGR J17091−3624 (King et al. 2012).

A broad Fe Kα line is also present, but our result indicates that the spin parameter of the source can only be weakly constrained under certain circumstances. However, if the corona is compact, as is generally assumed, we find an upper limit of $a^* \sim 0.5$, broadly consistent with the result of Hiemstra et al. (2011). Longer exposure and dynamic information would be extremely helpful in breaking the degeneracies between the spin and inclination, and allow a much tighter constraint in the spin parameter.

ACKNOWLEDGMENTS

REFERENCES

Bardeen J. M., Press W. H., Teukolsky S. A., 1972, ApJ, 178, 347
Bhattacharyya S., Strohmayer T. E., 2007, ApJ, 664, L103
Blum J. L., Miller J. M., Fabian A. C., Miller M. C., Homan J., van der Klis M., Cackett E. M., Reis R. C., 2009, ApJ, 706, 60
Brenneman L. W., Reynolds C. S., 2006, ApJ, 652, 1028
Brenneman L. W. et al., 2011, ApJ, 736, 103
Cackett E. M., Altamirano D., Patruno A., Miller J. M., Reynolds M., Linares M., Wijnands R., 2009a, ApJ, 694, L21
Cackett E. M. et al., 2009b, ApJ, 690, 1847
Cadolle Bel M. et al., 2007, ApJ, 659, 549
Chiang C.-Y., Fabian A. C., 2011, MNRAS, 414, 2345
Dauser T., Wilms J., Reynolds C. S., Brenneman L. W., 2010, MNRAS, 409, 1534
Davis S. W., Done C., Blaes O. M., 2006, ApJ, 647, 525
De Villiers J.-P., Hawley J. F., Krolik J. H., Hirose S., 2005, ApJ, 620, 878
di Salvo T. et al., 2009, MNRAS, 398, 2022
Fabian A. C., Rees M. J., Stella L., White N. E., 1989, MNRAS, 238, 729
Fabian A. C. et al., 2009, Nat, 459, 540
Gallo L. C., Fabian A. C., 2011, MNRAS, 418, L59
Garofalo D., 2009, ApJ, 699, 400
Garofalo D., Evans D. A., Sambruna R. M., 2010, MNRAS, 406, 975
Hiemstra B., Méndez M., Done C., Díaz Trigo M., Altamirano D., Casella P., 2011, MNRAS, 411, 137
Homan J., Wijnands R., van der Klis M., Belloni T., van Paradijs J., Klein-Wolt M., Fender R., Méndez M., 2001, ApJS, 132, 377
King A. L. et al., 2012, ApJ, 746, L20
Laor A., 1991, ApJ, 376, 90
McClintock J. E., Shafee R., Narayan R., Remillard R. A., Davis S. W., Li L., 2006, ApJ, 652, 518
Markwardt C. B., Swank J. H., Krimm H. A., Pereira D., Strohmayer T. E., 2009a, Astron. Telegram, 2107, 1
Markwardt C. B., Beardmore A. P., Miller J., Swank J. H., 2009b, Astron. Telegram, 2120, 1
Miller J. M., 2007, ARA&A, 45, 441
Miller J. M., Raymond J., Fabian A., Steeghs D., Homan J., Reynolds C., van der Klis M., Wijnands R., 2006, Nat, 441, 953
Miniutti G., Fabian A. C., Miller J. M., 2004, MNRAS, 351, 466
Miniutti G., Panessa F., de Rosa A., Fabian A. C., Malizia A., Molina M., Miller J. M., Vaughan S., 2009, MNRAS, 398, 255
Mitsuda K. et al., 1984, PASJ, 36, 741
Nardini E., Fabian A. C., Reis R. C., Walton D. J., 2011, MNRAS, 410, 1251
Pounds K. A., Reeves J. N., 2009, MNRAS, 397, 249
Pozdnyakov L. A., Sobol I. M., Syunyaev R. A., 1983, Astrophys. Space Phys. Rev., 2, 189
Proga D., Kallman T. R., 2002, ApJ, 565, 455
Reeves J. N. et al., 2009, ApJ, 701, 493
Reis R. C., Fabian A. C., Ross R. R., Miller J. M., 2009a, MNRAS, 395, 1257
Reis R. C., Fabian A. C., Young A. J., 2009b, MNRAS, 399, L1
Reis R. C., Fabian A. C., Miller J. M., 2010, MNRAS, 402, 836
Reis R. C. et al., 2011, MNRAS, 410, 2497
Remillard R. A., McClintock J. E., 2006, ARA&A, 44, 49
Ross R. R., Fabian A. C., 2005, MNRAS, 358, 211
Ross R. R., Fabian A. C., 2007, MNRAS, 381, 1697
Schmoll S. et al., 2009, ApJ, 703, 2171
Shimura T., Takahara F., 1995, ApJ, 445, 780
Steiner J. F., McClintock J. E., Remillard R. A., Narayan R., Gou L., 2009, ApJ, 701, L83
Tanaka Y. et al., 1995, Nat, 375, 659
Tchekhovskoy A., McKinney J. C., 2012, ArXiv e-prints
Tombesi F., Cappi M., Reeves J. N., Palumbo G. G. C., Yaqoob T., Braito V., Dadina M., 2010, A&A, 521, A57
Vaughan S., Fabian A. C., Ballantyne D. R., De Rosa A., Piro L., Matt G., 2004, MNRAS, 351, 193
Walton D. J., Reis R. C., Fabian A. C., 2010, MNRAS, 408, 601
Walton D. J., Reis R. C., Cackett E. M., Fabian A. C., Miller J. M., 2012, ArXiv e-prints
Zdziarski A. A., Lubiński P., Smith D. A., 1999, MNRAS, 303, L11
Zdziarski A. A., Poutanen J., Paciesas W. S., Wen L., 2002, ApJ, 578, 357
Zhang S. N., Cui W., Chen W., 1997, ApJ, 482, L155

This paper has been typeset from a TEX/LATEX file prepared by the author.